Lasers in Manufacturing Conference 2023

In-situ defect detection via active laser thermographic testing for PBF-LB/M

Philipp Peter Breese[a,*], Tina Becker[a], Simon Oster[a], Christian Metz[b], Simon J. Altenburg[a]

[a]*Bundesanstalt für Materialforschung und -prüfung (BAM), Unter den Eichen 87, 12205 Berlin, Germany*
[b]*THETASCAN GmbH, Thyssenstr. 183a, 46535 Dinslaken, Germany*

Abstract

Great complexity characterizes Additive Manufacturing (AM) of metallic components via laser powder bed fusion (PBF-LB/M). Due to this, defects in the printed components (like cracks and pores) are still common. Monitoring methods are commercially used, but the relationship between process data and defect formation is not well understood yet. Furthermore, defects and deformations might develop with a temporal delay to the laser energy input. The component's actual quality is consequently only determinable after the finished process.
To overcome this drawback, thermographic in-situ testing is introduced. The defocused process laser is utilized for nondestructive testing performed layer by layer throughout the build process. The results of the defect detection via infrared cameras are shown for a research PBF-LB/M machine.
This creates the basis for a shift from in-situ monitoring towards in-situ testing during the AM process. Defects are detected immediately inside the process chamber, and the actual component quality is determined.

Keywords: Additive Manufacturing; Laser Powder Bed Fusion; Nondestructive Testing; Thermography; Defect Detection

1. Introduction

The formation of defects in metal components is still a major issue for the Additive Manufacturing (AM) process of Laser Powder Bed Fusion (PBF-LB/M). Defect types include, among others, cracks, pores, and deformations among others. Different methods for monitoring the process exist, but process monitoring

* Corresponding author. Tel.: +49 30 8104 4670
E-mail address: philipp-peter.breese@bam.de

cannot replace a dedicated testing yet. The reason for this is twofold: on the one hand, the PBF-LB/M process is characterized by great complexity - e.g., due to short time scales and high temperature gradients. Big progress was made to relate data from monitoring to the resulting defects - e.g., using neural networks for porosity prediction (Oster et al., 2023). However, a definitive, holistic approach is not available yet. On the other hand, defect formation may occur with a delayed response to the energy and material deposition, e.g., due to thermal gradients and stress. Therefore, dedicated ex-situ testing (like X-ray computer tomography) after the finished process is still needed to determine the actual component quality. This obviously increases lead times and costs while rejects may not be found until ex-situ evaluation.

In this work, we present an approach to determine the actual component quality in situ and nondestructively during the process. By using active laser thermography, defects can be visualized due to their thermal contrast in response to local heating, recorded with an infrared (IR) camera. For the necessary heat input, the defocused process laser at low power level is utilized. So except for the required defocusing, no additional modifications on the machine are needed per se.

Within this work, we present intermediate results of the ZIM project *ATLAMP*. We investigated two scenarios using active laser thermography: a non-AM specimen with fine surface cracks (<10 µm width) placed within a PBF-LB/M process chamber, and a printed AM component with artificial notches during the actual PBF-LB/M process. Additional background on the thermographic testing method is provided initially. Afterwards, the experimental setup is described, the thermographic results for specimen and AM process are shown and discussed, and an outlook is given. The results mark a vital step towards implementing in-situ testing within the PBF-LB/M process.

2. Background on active laser thermographic testing

Active thermography (or active thermographic testing) is a nondestructive testing (NDT) technique that applies heat on the tested specimen surface to generate a non-stationary heat flux. This heat flux is hindered in defective regions, and a contrast to non-defective regions emerges (Kolb et al., 2021). It can be observed by monitoring the surface temperature development via an IR camera. As a specific method, the flying spot thermography introduces heat via a laser spot that travels across the tested surface. Its main application lies within detecting surface defects like cracks. These surface defects hinder the lateral heat propagation and result in a thermal contrast (Salazar, Mendioroz, and Oleaga, 2020).

In the context of PBF-LB/M, the in-situ usage of flying spot thermography is very limited until now. Herzer and Schilp, 2022 showed that detecting defects is possible using the process laser at reduced power. However, due to the small laser spot diameter, a nondestructive nature of the testing process could not be ensured. In a previous work (Breese et al., 2022), we showed that nondestructive flying spot thermography inside the process chamber is possible. For this, a non-AM test specimen with a notch was used while nondestructiveness was achieved via defocusing the process laser and finding suiting scanning parameters at high scanning speeds and low laser power. However, an application on the PBF-LB/M process was not shown yet. Hence, research is still needed to succefully implement nondestructive in-situ testing via active thermography for AM.

3. Experimental setup and methods

In this section, the PBF-LB/M research machine that was used for carrying out the experimental study as well as the infrared camera system are introduced.

3.1.1. PBF-LB/M research machine SAMMIE

To maximize controllability and data access, a custom PBF-LB/M research machine was realized. This Sensor-based Additive Manufacturing Machine (*SAMMIE*) was used for the research in this publication and is depicted in Fig. 1.

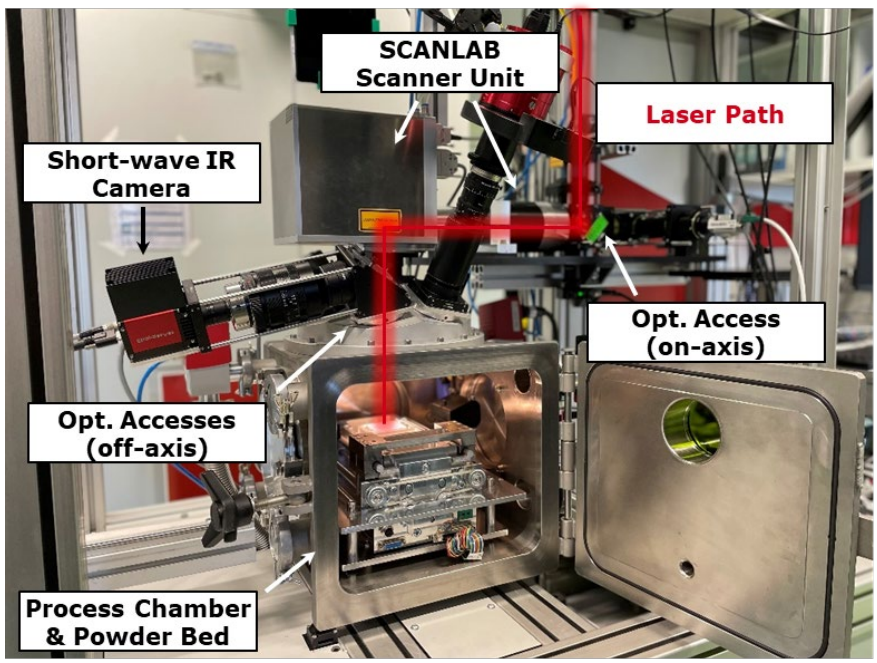

Fig. 1. Overview of the components of the PBF-LB/M research machine *SAMMIE*.

Fig. 1 shows the subcomponents of *SAMMIE* including the laser path with a focusing unit (varioSCAN by SCANLAB) and a galvanometer scanner (intelliSCAN by SCANLAB). The laser source is an ytterbium continuous wave fiber laser (IPG Photonics) emitting at 1070 nm with a maximum nominal output power of 500 W. Build job and laser path components are controlled via the Direct Machining Control (DMC) software. Furthermore, the process chamber with the powder bed unit is depicted. Due to four optical windows on the top, *SAMMIE* offers the possibility to install multiple camera systems simultaneously. The whole powder bed is observable with these off-axis configurations at the process chamber's optical accesses. Moreover, high spatial resolutions are achievable due to the short distance between optical windows and powder bed (ca. 220 mm). Furthermore, camera installations using the laser path (on-axis, also known as coaxial) can be realized as well (e.g., to monitor the melt pool at increased acquisition frequencies compared to the off-axis setup). However, this option was not used in this study, but is planned for future works. The powder bed, along with the whole PBF-LB/M process operation (e.g., vacuum system, inert gas and gas filtering system, additional sensors), is controlled by software realized in LabVIEW (National Instruments). With this, a fully

accessible PBF-LB/M process is feasible with *SAMMIE* while additional procedures like active laser thermographic testing are includable.

3.1.2. IR camera setup

For the thermographic data acquisition, a short-wave infrared (SWIR) camera (Goldeye CL-033 TEC1 by Allied Vision) was used (cf. also Fig. 1). Its spectral sensitivity ranges from 0.9 µm to 1.7 µm with the built-in InGaAs sensor. The image size at full frame is 640 by 512 px² at 14 bit image depth with a framerate of 234 Hz. The spectral range of SWIR was chosen since works with on-axis active laser thermography are planned for the future. The laser path is optimized for transmissivity at the laser wavelength of 1070 nm, but is still transmissive in the whole SWIR range. Therefore, SWIR assures a transfer to on-axis operation while for now, off-axis experiments investigate the general feasibility of the approach. Additionally, an in-process monitoring of the melt pool is possible as well while using the same SWIR camera setup. Also, SWIR cameras have a lower price compared to cooled mid-wave infrared cameras (MWIR) that are commonly used for thermographic testing.

The camera was equipped with a lens at a focal length of 100 mm. An extensions tube (length approximately 35 mm) was used in between to focus on the build plane. This resulted in a spatial resolution of 40 µm/px. Furthermore, a notch filter for the laser wavelength (NF1064-44 by Thorlabs) was installed in front of the camera objective. This ensured that solely the thermal response was recorded and not the reflected laser itself. The camera system was installed at one of the optical accesses of the *SAMMIE* process chamber via an adjustable mirror system. In this way, the alignment of recorded camera image and region of interest on the build plane was possible.

3.2. Laser thermography on test specimen

In the following, the setup for the preliminary experiments on a specimen with surface cracks is presented. This includes the specimen properties as well as the parameters for the active laser thermographic testing within the PBF-LB/M machine *SAMMIE*.

3.2.1. Specimen properties

Preliminary thermographic tests were carried out on a reference test specimen for magnetic particle inspection. It was used due to its various surface cracks (width 1 to 10 µm in the tested area). This makes it suitable for active laser thermographic testing via flying spot thermography. It is depicted in Fig. 2.

Fig. 2. Investigated surface cracks test specimen.

The specimen is made from 90MnCrV8 stainless steel and has a diameter of 50 mm and a width of 10 mm. It was hardened, pickled, and stress corrosion cracks were induced on its surface. The treatment gave the specimen a dark color. However, as shown in Fig. 2, the surface is not homogeneously colored which indicates inhomogeneous emissivity (and therefore absorptivity) of the specimen surface.

3.2.2. Testing parameters for the specimen

The test specimen was placed inside the process chamber of the PBF-LB/M machine *SAMMIE* for performing active laser thermography. Its surface was located at the height of the AM process build plane. Inside the process chamber, argon atmosphere similarly to the actual AM build process was established. The process laser was defocused for the testing sequence which resulted in a laser spot diameter of $D_{86} \approx 1.1$ mm. For the flying spot active laser thermography, an area of 5 by 4.8 mm² was scanned. An appropriate, nondestructive parameter set was found empirically at a laser power of 21 W and a scanning speed of 150 mm/s. Selecting a lower laser power was not possible as this marks the lower boundary for the used fiber laser model. The distance between scan tracks was 250 µm which resulted in a total of 20 scan tracks. The tracks were scanned monodirectionally with sky writing engaged to ensure constant scanning speeds during laser heat input. The whole testing sequence lasted 0.7 s which resulted in an energy input per area of 61 J/cm².

The SWIR camera was operated at an image size of 140 by 150 px² for capturing the whole scanning sequence. A setting with an exposure time of t_{exp} = 500 µs and an aperture of 5.6 made full use of the dynamic range of the detector. The frame rate was set to 1000 Hz.

3.3. Laser thermography during PBF-LB/M process

For a first proof of concept, the active laser thermography method was adapted to a PBF-LB/M build job. Flying spot laser thermography was performed in the AM research machine *SAMMIE* after every finished layer. The design of the build job along with the parameters for the thermographic testing are presented in the following.

3.3.1. Build job

The PBF-LB/M build job was performed with 316L stainless steel powder (1.4404) from SLM Solutions with particle sizes ranging from 10 to 45 µm (d_{50} = 32.55 µm). An inert gas atmosphere with argon was established and a continuous flow over the building area was ensured. For the tested component, a design with a total of six notches was created. It is depicted in 3D-Model of the built and tested AM component. The scan tracks of the thermographic testing are shown in white.Fig. 3 along with the scan tracks for the

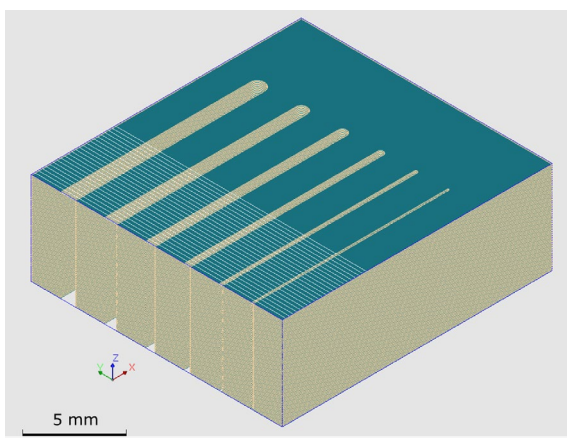

Fig. 3. 3D-Model of the built and tested AM component. The scan tracks of the thermographic testing are shown in white.

flying spot thermographic testing of the final layer (white).

The notches were chosen to mimic general characteristics of cracks and lack of fusion defects. They were implemented as unscanned areas with widths in µm of 1000, 800, 600, 400, 200, and 100. The complete component had a size of 18.4 by 17.1 mm² and a height of 6.28 mm. The layer height of 40 µm resulted in a total of 157 layers. The manufacturing was performed at a laser power of 167 W at 700 mm/s scanning speed. Sky writing was engaged, scans were performed monodirectionally, and a change of 67 degrees in scanning direction was included between layers. The hatching distance between scan vectors was set to 100 µm and the laser spot had a diameter (D_{86}) of approximately 80 µm.

3.3.2. Testing parameters for built component

For the flying spot laser thermography on the finished AM component layers, the process laser was defocused to reach a diameter of $D_{86} \approx 1.1$ mm. An area of 5.5 by 17.1 mm² was scanned (cf. Fig. 3), and the laser power was set to 32 W while the scanning speed was at 22 mm/s. Again, scanning was performed monodirectionally and sky writing was engaged. With a distance of 250 µm between scan vectors, a total of 23 laser tracks were performed. A total duration of 22.4 s for the tested region resulted in an energy per area of 762 J/cm². Testing took place automatically after each finished layer.

The SWIR camera was operated at full frame mode with 640 by 512 px². The exposure time was set to t_{exp} = 200 µs and the aperture to 22. The frame rate was set to 235 Hz due to the full frame setting.

3.4. Analysis of the laser thermography data

A typical method for analyzing flying spot thermographic data is finding and displaying the maximum value of the recorded thermal response for every pixel. This corresponds to every location during the NDT laser scanning. Additionally, the subsequently highest values after the maximum for every pixel may be found and sorted in descending order (Schlichting et al., 2012). This is done as the information content within a single frame during the thermographic testing is rather low and the testing sequence has to be analyzed as a whole. The exact time at which the respective values were reached do not matter in hindsight. This forms a sequence for the whole scanning area starting at the maximum value for every pixel. It is followed by lower values for every sequence step. This means that areas which retain higher values throughout the sequence, stayed at a higher temperature for a longer time. Vice versa, areas which drop to lower values faster in the sequence, cooled down faster or did not reach a high temperature. Information about local defects like cracks can be deducted from that. This data analysis makes localization and characterization possible of said defects which hinder the heat flux. It was applied on both presented instances: the surface crack specimen and the AM build job. Further processing like edge detection was not applied yet. For the AM build job, the full frame was cut as the second component in the image was not part of the investigations for this study.

4. Results and discussion

In the following, the results of the active laser thermography via flying spot are presented and discussed. This includes the in-situ testing of the surface cracks specimen and of the AM component with notches.

4.1. Laser thermography on test specimen

As described in section 3.4, the recorded values for the surface's thermal response were sorted from the maximum for every pixel. A frame from the resulting sequence is shown in Fig. 4 (a).

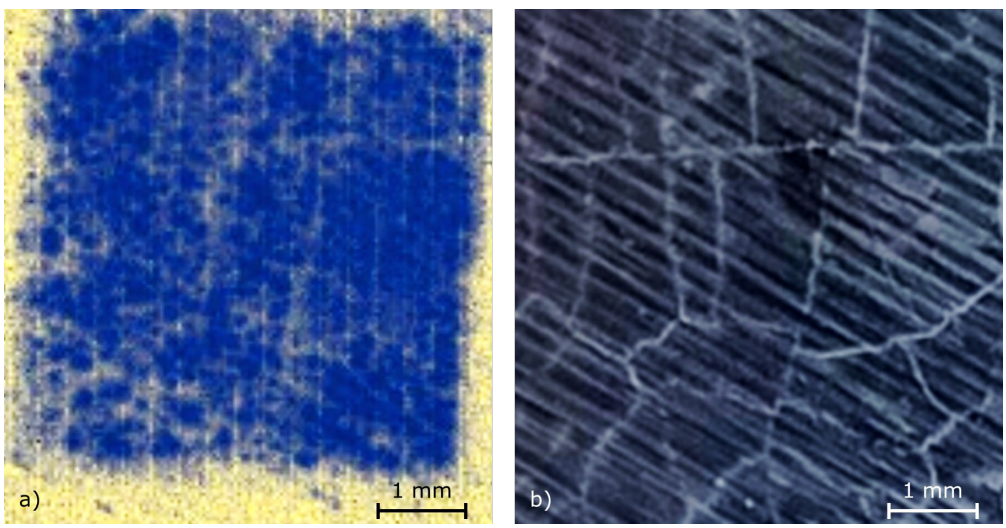

Fig. 4. (a) Single frame of the resulting sequence based on the active laser thermography data; (b) Photography of the same region with lighting conditions that make the surface cracks visible.

The shape of the cracks is recognizable in the thermographic image. However, no sharp boundaries are observable. For comparison purposes, Fig. 4 (b) shows a photography of the same surface region. Under the right lighting conditions, the cracks may be visible as shown here. The comparison makes clear that the laser thermography inside the AM process chamber has the potential to detect even small surface cracks. However, the test result shows that not all defects could be detected - presumably, due to the given limitations of the used setup. These limitations include the fixed minimum laser power and the fixed maximum laser spot diameter. At lower laser power with a bigger spot, parameters would come closer to typical settings for flying spot thermography. This left the scanning speed as the last method to influence the energy input for the laser thermography. Combined with the dark (high laser absorptivity) and inhomogeneous surface of the specimen, the scanning speed could not be reduced further than the chosen 150 mm/s to ensure nondestructiveness (NDT). For upcoming experiments, tests of AM components with natural surface cracks at similar sizes are planned.

The presented results suggest that finding small cracks in this scenario is very plausible. Furthermore, an extension towards longer wavelengths for the camera would most likely improve results. However, usability for on-axis applications along with possibly higher camera prices must be taken into account.

4.2. Laser thermography during PBF-LB/M process

For the flying spot thermography of the AM component during the process, a higher energy input is feasible (32 W at 22 mm/s) compared to the surface cracks test specimen (21 W at 150 mm/s). A new nondestructive parameter set had to be found empirically as much higher energy per area is possible here before destruction takes place. A main reason for this is the lower laser absorptivity of the AM component surface compared to the reworked test specimen surface. More energy per area is needed for the same temperature rise. However, when recording the thermal response with the IR camera, the lower emissivity across the SWIR range must be considered for the camera setup.

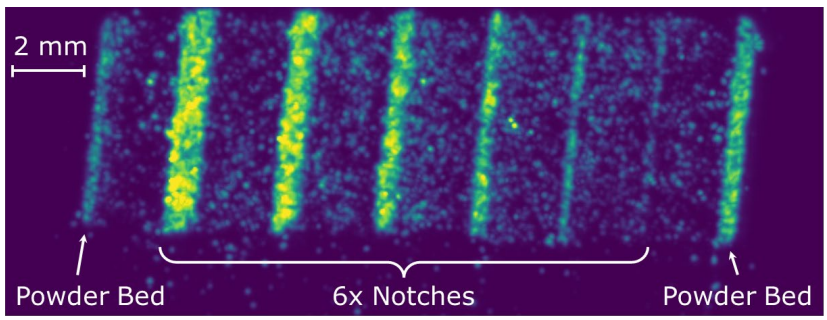

Fig. 5. Result of the thermographic testing via flying spot for layer 142.

The pixel-wise maximum thermogram created from the recorded flying spot thermography data of layer 142 of the PBF-LB/M process is shown in Fig. 5. All six notch structures are discernible in the image. Even the smallest notch at a nominal width of 100 µm can be detected, even though its actual width is most probably smaller due to an expanded area of powder melting. The good visibility stems from the interaction between defocused laser and powder located inside the notches. The powder's absorptivity (and therefore also emissivity) is higher compared to the surrounding solidified material. It most probably reaches a higher temperature than the solid material. Furthermore, it stays at a higher temperature for a longer time than the solid material. Heat conduction is reduced in the powder which is observable in the thermogram sequence. These effects also explain the reduced notch visibility with reduced notch width. With less powder volume and the solid material directly nearby, temperatures do not rise as high and fall faster. Fig. 5 also shows the edges of the component to the powder bed. This is due to the thermal response as the defocused laser not only scans over the component surface, but also slightly into the powder bed. This may be used in the future to determine the actual position of the built AM component inside the machine.

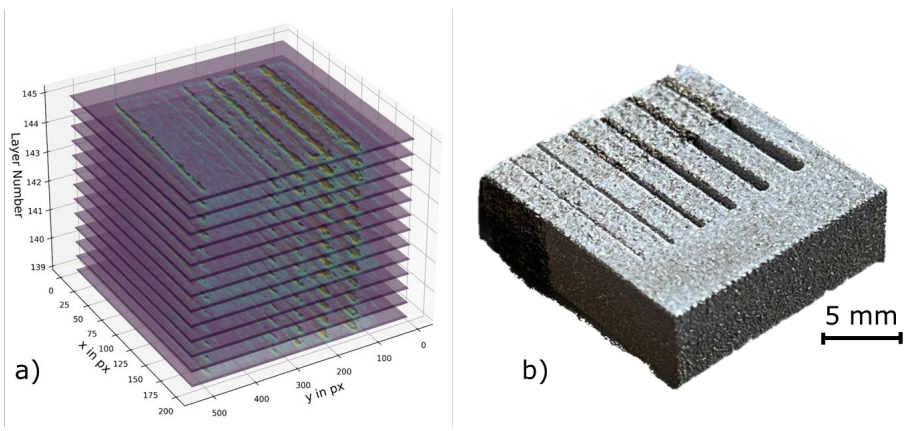

Fig. 6. (a) 3D visualization of the layers during the PBF-LB/M process tested via flying spot thermography; (b) Finished component with visible marks from flying spot thermography.

The flying spot thermography scan was carried out after each manufactured layer. A 3D view of the resulting maximum thermograms is shown in Fig. 6 (a) for the layers 139 to 145. Thus, nondestructive testing can be performed throughout the whole build process if needed. Defects may be found immediately, and appropriate measures may be performed. However, as observable in the image of the finished component (Fig. 6 (b)), the heat input of the thermographic testing still influences the AM component itself. The powder gets sintered inside the notches where testing took place. Furthermore, a slight darkening of the AM component surface is visible, so the flying spot parameters have to be optimized further. However, it is imaginable that an additional heat input may even be beneficial for the component quality, but studies on this aspect are necessary. Nevertheless, the implementation of active laser thermographic testing of each layer during the PBF-LB/M process shows potential for a future with in-situ nondestructive testing for AM.

5. Summary and outlook

Within this work, we investigated the possibility of detecting surface defects by applying in-situ NDT in the Additive Manufacturing process PBF-LB/M. To this end, flying spot thermography was used. The required heat input was realized with the defocused process laser at low power levels and the thermal response was recorded with an off-axis SWIR camera. Two scenarios were investigated: Firstly, a stainless steel test specimen with natural surface cracks was tested. The thermographic testing within the PBF-LB/M process chamber verified that detecting cracks with low widths (< 10 µm) is possible with the used setup. However, initial results show the potential of improvements due to limiting factors (camera wavelength, minimum laser power, maximum spot diameter, surface properties etc.). Nonetheless, it still has to be considered that this kind of dark and reworked surface is only poorly comparable to solidified AM surfaces, and the results gave good insights on what to consider for optimizing outcomes. Secondly, an AM component was tested during the PBF-LB/M process by performing laser thermography on each finished layer by an automated in-situ testing procedure. The artificially introduced notch areas were detectable even at the lowest width of 100 µm. The unmelted powder in the notch areas gave a high thermal contrast, and the actual component status was assessable. However, even with the defocused laser at low power, the powder was sintered, and further optimization of the testing parameters might be needed. The influence of this effect on the AM component quality along with the impact of additional heat input has to be investigated in future studies. The use of a camera sensitive at longer wavelengths would enable the detection of lower surface temperatures, giving the opportunity to further reduce the laser heat input to avoid powder sintering. Thus, this approach will be investigated in future studies. Although a few open questions remain, the goal of replacing ex-situ testing with in-situ laser thermography appears to be in reach.

Acknowledgements

The project *ATLAMP* is supported by the Federal Ministry for Economic Affairs and Climate Action (BMWK) on the basis of a decision by the German Bundestag. Grant numbers - BAM: 16KN086124; THETASCAN GmbH: 16KN086125.

References

Breese, P. P., Becker, T., Oster, S., Altenburg, S. J., Metz, C., Maierhofer, C., 2022. Aktive Laserthermografie im L-PBF-Prozess zur in-situ Detektion von Defekten. DGZfP-Berichtsband.

Herzer, F., Schilp, J., 2022. Detektion von Bindefehlern durch Laser-Thermografie beim pulverbettbasierten Schmelzen von Metallen mittels Laserstrahl. DGZfP-Berichtsband.

Kolb, C. G., Zier, K., Grager, J.-C., Bachmann, A., Neuwirth, T., Schmid, S., Haag, M., Axtner, M., Bayerlein, F., Grosse, C. U., Zaeh, M. F., 2021. An investigation on the suitability of modern nondestructive testing methods for the inspection of specimens manufactured by laser powder bed fusion. SN Applied Sciences.

Oster, S., Breese, P. P., Ulbricht, A., Mohr, G., Altenburg, S. J., 2023. A deep learning framework for defect prediction based on thermographic in-situ monitoring in laser powder bed fusion. Journal of Intelligent Manufacturing.

Salazar, A., Mendioroz, A., Oleaga, A., 2020. Flying spot thermography: Quantitative assessment of thermal diffusivity and crack width. Journal of Applied Physics.

Schlichting, J., Ziegler, M., Maierhofer, C., Kreutzbruck, M., 2012. Flying Laser Spot Thermography for the Fast Detection of Surface Breaking Cracks. 18th World Conference on Nondestructive Testing.